Int. J. Pharm. Investigation, 2026; 16(2):654-666.
https://www.jpionline.org

Original Article

# Computational Tool and Molecular Properties to Identify the Molecular Targets of Novel Benzimidazole Derivatives as Potential COX Inhibitors via *in silico* Approaches

**Vinod Rajendra Tawate[1], Sanket Keshav Tambe[1], Shubham Popatrao Mankar[1], Nilima Mahesh Wani[1], Sneha Abhishek Vikhe[2], Manisha Dhondiram Sonawane[1], Rohit Jaysing Bhor[1,*]**

[1]Department of Pharmaceutical Chemistry, Pravara Rural College of Pharmacy, Pravaranagar, Rahata, Ahmednagar, Maharashtra, INDIA.
[2]Department of QA, Pravara Rural College of Pharmacy, Pravaranagar, Rahata, Ahmednagar, Maharashtra, INDIA.

## ABSTRACT

**Background:** Using a variety of computational techniques, *in silico* studies allow for forecasting structural changes and how they would impact the pharmacological properties as well as the efficiency of these modifications. The computational study of benzimidazole derivatives is the main topic of this article. All compounds' cytotoxicity against inflammation was assessed, and the outcomes showed that several of them had strong inhibitions. This study investigates the many pharmacological characteristics of benzimidazole derivatives, including their anticancer, antibacterial, antioxidant, anti-inflammatory, and anticonvulsant effects. The proposed approach summarizes each activity *in silico* research. The structure-activity correlations and pharmacological effects of compounds containing benzimidazole are examined in this study. **Materials and Methods:** Molecular Design Suite was used to conduct Combi Lab investigations and 3D-QSAR. Schrodinger Maestro was used for the molecular docking investigation. **Results:** Seven compounds (VT1 and VT16) in a library of 16 compounds created using a combinatorial approach demonstrated superior projected biological activity than the dataset's most active molecule. These chemicals exhibited proximal contact with amino acid residues on COX-2 such as TYR355 and/or ARG120. **Conclusion:** This study determined the structural elements affecting by carefully changing the substituents, ring modifications, and linker groups. The logical creation and optimization of more powerful and selective molecules is made possible by these discoveries. In contrast to the reference ligand, the current study produced more powerful benzimidazoles as inhibiting compounds for COX-2 with excellent interaction. The study's findings could aid in the creation of new COX-2 inhibitors to treat inflammatory conditions.

**Keywords:** Inflammation, ADMET, Benzimidazole, Molecular docking, COX 1, COX 2.

**Correspondence:**
**Dr. Rohit Jaysing Bhor**
Department of Pharmaceutical Chemistry, Pravara Rural College of Pharmacy Pravaranagar, B-10, Lane 2, Musale vasti, Hasanapur road, Loni (B.K.), Rahata, Ahmednagar, Maharashtra, INDIA.
Email: rohit.bhor69@gmail.com
ORCID: 0000-0002-7979-3765

**Received:** 22-08-2025;
**Revised:** 06-10-2025;
**Accepted:** 19-12-2025.

## INTRODUCTION

The combination of imidazole with benzene results in the heterocyclic aromatic organic molecule known as benzimidazole. Because of their many effects, i.e., analgesic, anti-tumor, antiviral, and psychoactive properties, they have played a significant role in medicinal chemistry (Ayeni *et al*., 2022). The intricate biological reaction of bodily tissues to infections, which is defensive action towards immune cells (Bomalaski *et al*., 2000). Cyclooxygenase (COX), which comes in the forms COX-1 and 2, is essential protein needed for convert arachidonic acid to prostaglandins. Prostaglandins are supplied by COX-1, while COX-2 is produced subsequent to inflammatory stimuli (Bortoli *et al*., 2019). In human cancers, COX-2 contributes to angiogenesis as well as cell division and death. One technique for figuring out how a protein and ligand interact is called molecular docking, and it explains the molecule's orientation, binding interactions, and binding energy (Chen *et al*., 2018). Predicting the shared molecular characteristics those in molecular interactions with biological target and initiate response requires the use of pharmacophore methods. The purpose of this investigation was to determine the molecular interactions in benzimidazoles analogues and COX, as well as to screen the synthetic compounds' physicochemical and ADMET characteristics (Das *et al*., 1995). Additionally, pharmacophore modelling studies were used to examine distinctive traits. Since the benzimidazole derivatives have been shown to have anti-inflammatory properties, it is necessary to demonstrate how they work (Durand *et al*., 1992). To ascertain these compounds *in silico* inhibitory effect, were docked with COX-1 (PDB: 2OYE) and COX-2 (PDB: 4COX). As a result, *in silico* research helps identify how benzimidazoles work to block

**DOI:** 10.5530/ijpi.20260528

**Copyright Information :**
Copyright Author (s) 2026 Distributed under Creative Commons CC-BY 4.0

**Publishing Partner :** Manuscript Technomedia. [www.mstechnomedia.com]

COX enzymes, which is what gives them their anti-inflammatory properties. Inflammation is a vital defensive mechanism against all forms of physical, chemical, and viral assault (García-lópez *et al.*, 2021). When this mechanism is dysregulated, the body develops pathological conditions, such as organ rejection, autoimmune diseases, and allergies (Hasanvand *et al.*, 2018). Since NSAID show lowering fever, inflammation, and pain, millions of patients use them all over the world. NSAIDs function pharmacologically by blocking the actions of COX, which stops enzymatic biotransformation of arachidonic acid into related pro-inflammatory prostaglandins and Thromboxane (TXs). Needleman and Isakson originally described two cyclooxygenase isoenzymes in 1997 (Hoehns *et al.*, 2018). The "House Keeping" enzyme, COX1, regulates a basic level of PGs for homeostasis preservation, including intestinal integrity. The "Inducible" enzyme, COX-2, causes inflammatory reactions and is triggered by a variety of events. It is currently unclear what the exact roles of a COX-3 isoform that is solely expressed in particular brain and spinal cord areas are. The second COX type (COX-2) produced in pathogenic and pro-inflammatory stimuli, including cytokines, lipopolysaccharides, and phorbol esters. COX2 is responsible for both PGs release and the inflammation. Numerous studies have linked COX-2 to a range of clinical illnesses, such as cancer, neurological disorders, and inflammation (Holm and Goa, 2000). As a result, also used in cancer treatment. In order to mitigate these serious side effects, selective COX-2 inhibitor medications i.e., celecoxib, rofecoxib, and valdecoxib were created (Jia *et al.*, 2000). These medications have analgesic property same as non-selective COX inhibitors, but they also have improved gastric safety profiles (Figure 2). Unfortunately, as they have adverse effects on COX pathway, which include an elevated risk of myocardial infarction and high blood pressure, valdecoxib and rofecoxib have both been removed from the market. The distinct chemical makeup of valdecoxib and rofecoxib was associated with their adverse effects (Lamptey *et al.*, 2000). As a result, research for selective anti-inflammatory medications with superior safety profiles than the NSAIDs on the market is still ongoing (Langtry *et al.*, 1990). In COX-1/COX-2 activity of inhibition synthesized derivatives was evaluated (Miao *et al.*, 2023). Lastly, the synthesized compounds docked into COX-2 site to clarify their possible method of action.

## MATERIALS AND METHODS

Autodock Vina was used to realize the docking process, while Discovery Studio 3.5 was used to visualize the interactions. Celecoxib (CEL) crystal structures were compared to the anticipated conformations of docking data in order to optimize the docking method. Figure 1 showed the superimposition of the crystallized form of the Ribbon Structure Protein structure and Ramachandran Plot. Figure 2 showed that scheme of Benzimidazole. The Protein Data Bank supplied the Ribbon Structure structures for COX-1 (PDB: 2OYE) and COX-2 (PDB: 4COX). Auto dock version was 1.5.6. Chain A was chosen. Polar hydrogens and Gasteiger charges were then introduced after the water was removed. They decided on a grid map. The compounds' 2D formula was drawn using ChemDraw Ultra 12.0. Avogadro software was used to minimize energy use.

### Molecular Docking and Ligand preparation

Preceding molecular docking, test compounds VT1-VT16 structures benzimidazole derivatives were given in Table 1. We optimized by using the semi-empirical approach and the ArgusLab 4.0.1 software program. Getting proteins ready We used a variety of different COX-1 and COX-2 enzyme crystal structures via the RCSB for docking studies.

### Modelling platform

Maestro 11.9 was used for all computational analysis. Software were installed on Dell Inc. 27-inch computer that was on Linux x86_64 as OS and has Intel Core i7-7700 CPU at 3.60 GHz x8 with 8GB RAM and 1000 GB HDD. Drug likeness, physicochemical characteristics, and ADMET of compounds were studied.

## RESULTS

ADMET (which stands for absorption, distribution, excretion, and toxicity) characteristics for substances are necessary to create effective oral medications. The toxicity of a ligand is thought to be required to ligand as function to effective discovery tool, and Qik-Prop produces physically relevant descriptions. The Ligprep module used for ligand preparation utilized in investigation. The protein preparation wizard utilized for protein preparation. The PDB data bank provided the X-ray crystal structures of COX-1 (PDB:2OYE) and COX-2 (PDB:4COX). The grid generated using Receptor Grid Generation Wizard. Glide XP coupled the ligand with the protein, and the interactions were seen. Based on the optimal ligand-protein interaction, the scoring function assigns points. The extra-precision mode was used to assess the docking positions. The program detects steric conflicts, metal-ligation interactions, hydrophobic interactions, and hydrogen bonding. Every substance has a molecular weight between 400 and 500, which is less than 500. The compounds' computed log *p* values fall between 2.56-4.35. The substances being studied have donors of hydrogen bonds. Two COX enzymes were docked with the drugs, and the molecular interactions between them were examined. Table 4 shows the calculated and tabulated docking scores and binding energy. Tables 4 summarize interactions between chemicals with residues of dynamic amino acids, whereas Figures 3 and 4 display the 2D-3D conformations for molecular bindings. Computer-Aided Molecular Design (CAMD) has traditionally concentrated on lead optimization and identification, and several creative techniques have been created to help increase the binding affinities of drug candidates to certain receptors. QSAR is one such technique that was covered in the previous chapter. This chapter will cover the newly developed idea of

"drug-likeness" as well as the computer modelling of a number of biological and physicochemical characteristics that are crucial in turning a clinical lead into a commercially available medication. Pharmacologists and medicinal chemists have looked for beneficial drug-like chemical characteristics that produce agents with predictable oral therapeutic effectiveness. Drug development process follows Lipinski's "rule of five" which is computational and experimental method for estimating solubility, permeability. Those are general guideline which assesses drug-likeness and establishes whether molecule has pharmacological activity. The rule was founded on the finding that the majority of medications that work well when taken orally are tiny, somewhat lipophilic molecules. It is employed in the process of developing new drugs when pharmacologically active lead structures are gradually improved to boost their activity and selectivity while maintaining their drug-like physicochemical characteristics. Bonds rotation; H-bond acceptors; H-bond donors; Lipinski; Ghose; Veber; Egan and Muegge violations were given in Table 2. Good ADMET

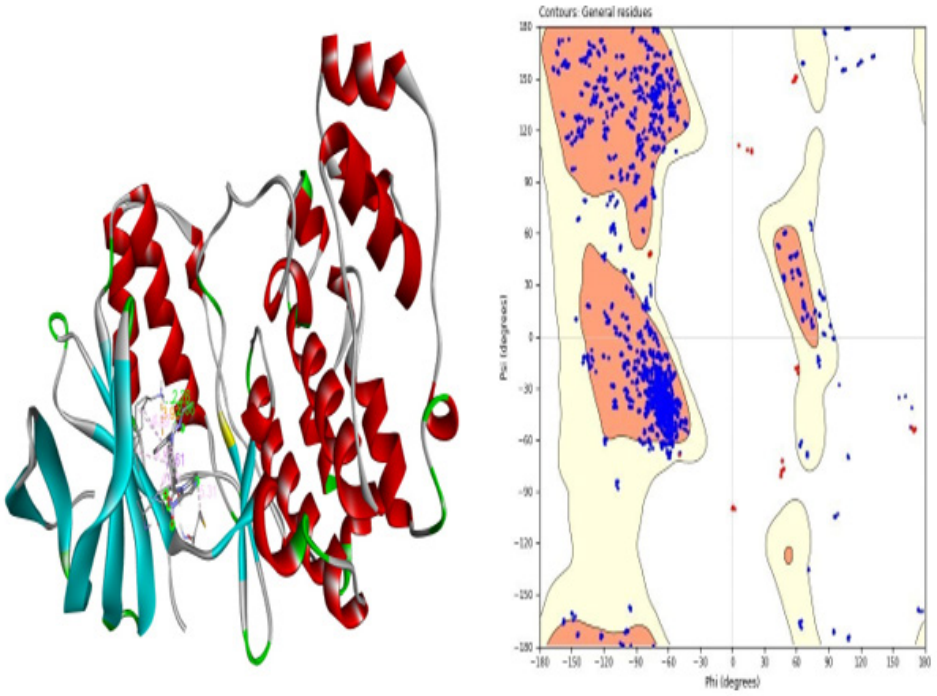


**Figure 1:** Ribbon Structure Protein structure and Ramachandran Plot.

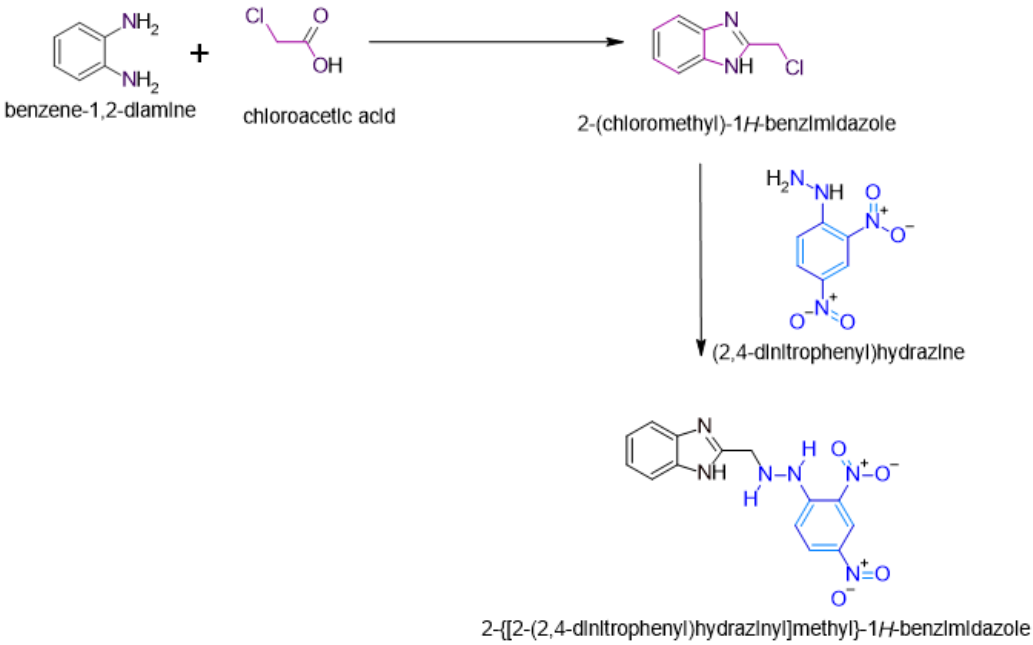


**Figure 2:** Scheme of Benzimidazole.

**Table 1: Derivatives of designed compound of Benzimidazole.**

| Comp. code | structure | Comp. code | structure |
|---|---|---|---|
| VT1 | 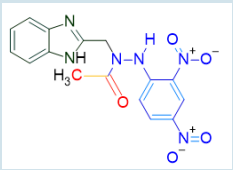 | VT9 | 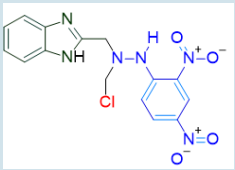 |
| VT2 | 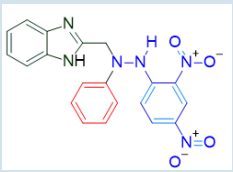 | VT10 | 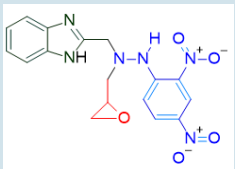 |
| VT3 | 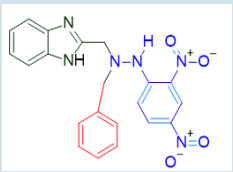 | VT11 | 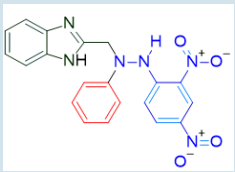 |
| VT4 | 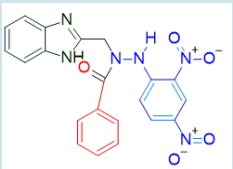 | VT12 | 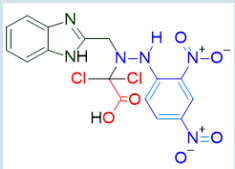 |
| VT5 | 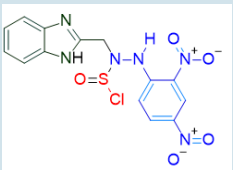 | VT13 | 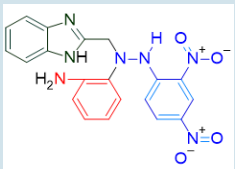 |
| VT6 | 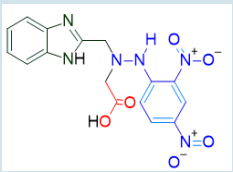 | VT14 | 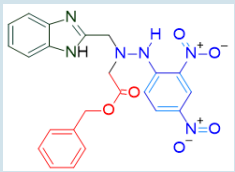 |
| VT7 | 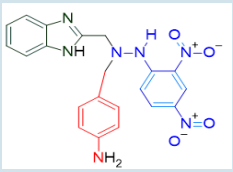 | VT15 | 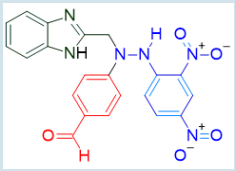 |
| VT8 | 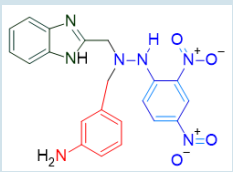 | VT16 | 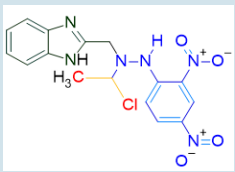 |

property prediction techniques are becoming more and more necessary to achieve two main goals. In order to lower the risk, novel compounds libraries should be designed first. Secondly, screening and testing should be optimized by focusing on the most promising compounds. Predicting characteristics like oral absorption, bioavailability, BBB penetration, clearance, and Vd (for frequency) which give information about dosage quantity and frequency is our goal. Molecular modelling and data modelling are the two categories of computational techniques that are employed. Molecular modelling utilizes quantum techniques to evaluate possibility of interaction, including cytochrome P450s, which has role in ADME processes. QSAR techniques is

**Table 4: Chemical interactions between the chemicals and the residues of active amino acids.**

| Name | Distance | Category | Type | Docking score |
|---|---|---|---|---|
| VT1 | | | | |
| | | | | -9.49 |
| C:TYR385 | 4.80335 | Hydrophobic | Pi-Pi T-shaped | |
| C:TRP387 | 4.90174 | Hydrophobic | Pi-Pi T-shaped | |
| C:TRP387 | 5.71241 | Hydrophobic | Pi-Pi T-shaped | |
| C:LEU352 | 4.81093 | Hydrophobic | Pi-Alkyl | |
| C:VAL349 | 4.73926 | Hydrophobic | Pi-Alkyl | |
| C:ALA527 | 4.08969 | Hydrophobic | Pi-Alkyl | |
| C:LEU531 | 5.36478 | Hydrophobic | Pi-Alkyl | |
| C:VAL349 | 4.73926 | Hydrophobic | Pi-Alkyl | |
| VT2 | | | | -5.307 |
| C:LEU352 | 5.02138 | Hydrophobic | Pi-Alkyl | |
| C:ALA516 | 5.15123 | Hydrophobic | Pi-Alkyl | |
| C:VAL523 | 3.81626 | Hydrophobic | Pi-Alkyl | |
| C:VAL523 | 3.827 | Hydrophobic | Pi-Alkyl | |
| C:ALA527 | 3.96014 | Hydrophobic | Pi-Alkyl | |
| C:LEU352 | 5.45723 | Hydrophobic | Pi-Alkyl | |
| C:ALA527 | 4.44987 | Hydrophobic | Pi-Alkyl | |
| | | | | |
| VT3 | | | | -8.361 |
| C:TYR385 | 3.89824 | Electrostatic | Pi-Cation | |
| C:ARG120:NH1 | 4.02048 | Electrostatic | Pi-Cation | |
| C:TYR385 | 3.24236 | Electrostatic | Pi-Anion | |
| C:SER353:HA | 2.42754 | Hydrophobic | Pi-Sigma | |
| C:TYR385 | 5.44301 | Hydrophobic | Pi-Pi T-shaped | |
| C:TRP387 | 5.11714 | Hydrophobic | Pi-Pi T-shaped | |
| C:VAL116 | 4.93057 | Hydrophobic | Pi-Alkyl | |
| C:VAL349 | 4.81653 | Hydrophobic | Pi-Alkyl | |
| - C:VAL349 | 5.46219 | Hydrophobic | Pi-Alkyl | |
| C:LEU359 | 4.84215 | Hydrophobic | Pi-Alkyl | |
| C:ALA527 | 3.47718 | Hydrophobic | Pi-Alkyl | |
| C:ALA527 | 4.89167 | Hydrophobic | Pi-Alkyl | |
| C:LEU531 | 5.38596 | Hydrophobic | Pi-Alkyl | |
| C:LEU531 | 4.83624 | Hydrophobic | Pi-Alkyl | |
| C:VAL523 | 3.64573 | Hydrophobic | Pi-Alkyl | |
| VT4 | | | | |
| C:SER530:HB2 | 2.93249 | Hydrogen Bond | Carbon Hydrogen Bond | -9.498 |
| C:MET522:SD | 4.9468 | Other | Pi-Sulfur | |
| C:PHE518 | 5.76057 | Hydrophobic | Pi-Pi Stacked | |
| C:TYR385 | 4.90608 | Hydrophobic | Pi-Pi T-shaped | |

| Name | Distance | Category | Type | Docking score |
|---|---|---|---|---|
| C:TRP387 | 5.11878 | Hydrophobic | Pi-Pi T-shaped | |
| C:GLY526:C,O;ALA527:N | 4.17467 | Hydrophobic | Amide-Pi Stacked | |
| C:GLY526:C,O;ALA527:N | 4.06391 | Hydrophobic | Amide-Pi Stacked | |
| C:ALA527 | 4.76414 | Hydrophobic | Pi-Alkyl | |
| C:LEU352 | 5.03924 | Hydrophobic | Pi-Alkyl | |
| C:VAL523 | 3.91752 | Hydrophobic | Pi-Alkyl | |
| C:VAL116 | 5.14071 | Hydrophobic | Pi-Alkyl | |
| C:VAL349 | 5.20555 | Hydrophobic | Pi-Alkyl | |
| C:LEU359 | 5.10366 | Hydrophobic | Pi-Alkyl | |
| C:ALA527 | 4.59914 | Hydrophobic | Pi-Alkyl | |
| C:LEU531 | 4.27988 | Hydrophobic | Pi-Alkyl | |
| VT5 | | | | -7.668 |
| C:ARG120:NH1 | 4.09516 | Electrostatic | Pi-Cation | |
| C:MET522:SD | 4.81724 | Other | Pi-Sulfur | |
| C:MET522:SD | 5.53783 | Other | Pi-Sulfur | |
| C:TYR385 | 4.50395 | Hydrophobic | Pi-Pi T-shaped | |
| C:TRP387 | 4.89647 | Hydrophobic | Pi-Pi T-shaped | |
| C:TRP387 | 5.48989 | Hydrophobic | Pi-Pi T-shaped | |
| C:TRP387 | 5.51741 | Hydrophobic | Pi-Pi T-shaped | |
| C:GLY526:C,O;ALA527:N | 4.40085 | Hydrophobic | Amide-Pi Stacked | |
| C:GLY526:C,O;ALA527:N | 4.50959 | Hydrophobic | Amide-Pi Stacked | |
| C:VAL349 | 4.64693 | Hydrophobic | Pi-Alkyl | |
| C:ALA527 | 3.61449 | Hydrophobic | Pi-Alkyl | |
| C:LEU531 | 4.97731 | Hydrophobic | Pi-Alkyl | |
| VT6 | | | | -7.318 |
| C:TYR385 | 5.26214 | Hydrophobic | Pi-Pi T-shaped | |
| C:TYR385 | 4.70811 | Hydrophobic | Pi-Pi T-shaped | |
| C:TRP387 | 5.13438 | Hydrophobic | Pi-Pi T-shaped | |
| C:TRP387 | 4.93085 | Hydrophobic | Pi-Pi T-shaped | |
| C:TRP387 | 5.4749 | Hydrophobic | Pi-Pi T-shaped | |
| C:LEU352 | 5.32918 | Hydrophobic | Pi-Alkyl | |
| C:LEU384 | 5.42378 | Hydrophobic | Pi-Alkyl | |
| C:MET522 | 5.08452 | Hydrophobic | Pi-Alkyl | |
| C:LEU352 | 5.34115 | Hydrophobic | Pi-Alkyl | |
| C:VAL523 | 3.8457 | Hydrophobic | Pi-Alkyl | |
| C:ALA527 | 5.32064 | Hydrophobic | Pi-Alkyl | |

| Name | Distance | Category | Type | Docking score |
|---|---|---|---|---|
| VT7 | | | | -8.468 |
| C:HIS90:NE2 | 2.02572 | Hydrogen Bond | Conventional Hydrogen Bond | |
| C:SER353:O | 2.92133 | Hydrogen Bond | Conventional Hydrogen Bond | |
| C:SER530:HG | 2.88367 | Hydrogen Bond | Conventional Hydrogen Bond | |
| C:ALA527:HA | 2.40724 | Hydrogen Bond | Carbon Hydrogen Bond | |
| C:SER530:HB1 | 2.92136 | Hydrogen Bond | Carbon Hydrogen Bond | |
| C:SER530:HB1 | 2.98681 | Hydrogen Bond | Carbon Hydrogen Bond | |
| C:ARG120:NH1 | 3.81245 | Electrostatic | Pi-Cation | |
| C:SER353:HA | 2.4381 | Hydrophobic | Pi-Sigma | |
| C:TYR385 | 4.89697 | Hydrophobic | Pi-Pi T-shaped | |
| C:TRP387 | 4.92733 | Hydrophobic | Pi-Pi T-shaped | |
| C:TRP387 | 5.8065 | Hydrophobic | Pi-Pi T-shaped | |
| C:LEU352 | 4.72345 | Hydrophobic | Pi-Alkyl | |
| C:VAL349 | 5.05276 | Hydrophobic | Pi-Alkyl | |
| C:ALA527 | 3.85135 | Hydrophobic | Pi-Alkyl | |
| C:LEU531 | 5.23398 | Hydrophobic | Pi-Alkyl | |
| C:VAL523 | 3.6578 | Hydrophobic | Pi-Alkyl | |
| VT8 | | | | -8.192 |
| C:TYR385 | 5.90289 | Hydrophobic | Pi-Pi T-shaped | |
| C:LEU352 | 4.99974 | Hydrophobic | Pi-Alkyl | |
| C:ALA516 | 5.22083 | Hydrophobic | Pi-Alkyl | |
| C:VAL523 | 3.84935 | Hydrophobic | Pi-Alkyl | |
| C:VAL523 | 3.80579 | Hydrophobic | Pi-Alkyl | |
| C:ALA527 | 4.81469 | Hydrophobic | Pi-Alkyl | |
| C:VAL349 | 5.27268 | Hydrophobic | Pi-Alkyl | |
| C:ALA527 | 3.73042 | Hydrophobic | Pi-Alkyl | |
| VT9 | | | | -6.673 |
| C:TYR385 | 5.28522 | Hydrophobic | Pi-Pi T-shaped | |
| C:TRP387 | 5.14247 | Hydrophobic | Pi-Pi T-shaped | |
| C:VAL523 | 3.47235 | Hydrophobic | Alkyl | |
| C:LEU352 | 4.368 | Hydrophobic | Pi-Alkyl | |
| C:VAL523 | 5.38985 | Hydrophobic | Pi-Alkyl | |
| C:VAL349 | 4.8152 | Hydrophobic | Pi-Alkyl | |
| C:LEU359 | 5.38903 | Hydrophobic | Pi-Alkyl | |
| C:ALA527 | 4.35198 | Hydrophobic | Pi-Alkyl | |

| Name | Distance | Category | Type | Docking score |
|---|---|---|---|---|
| VT10 | | | | -7.005 |
| C:TYR385 | 4.23927 | Electrostatic | Pi-Cation | |
| C:ARG120:NH1 | 3.82938 | Electrostatic | Pi-Cation | |
| C:TYR385 | 3.12232 | Electrostatic | Pi-Anion | |
| C:MET522:SD | 5.71089 | Other | Pi-Sulfur | |
| C:TRP387 | 5.40654 | Hydrophobic | Pi-Pi T-shaped | |
| C:VAL116 | 4.75028 | Hydrophobic | Pi-Alkyl | |
| C:VAL349 | 5.2154 | Hydrophobic | Pi-Alkyl | |
| C:LEU359 | 4.8858 | Hydrophobic | Pi-Alkyl | |
| C:ALA527 | 4.99105 | Hydrophobic | Pi-Alkyl | |
| C:ALA527 | 3.71016 | Hydrophobic | Pi-Alkyl | |
| C:LEU531 | 5.122 | Hydrophobic | Pi-Alkyl | |
| C:LEU352 | 5.29007 | Hydrophobic | Pi-Alkyl | |
| VT11 | | | | -5.307 |
| C:LEU352 | 5.02138 | Hydrophobic | Pi-Alkyl | |
| C:ALA516 | 5.15123 | Hydrophobic | Pi-Alkyl | |
| C:VAL523 | 3.827 | Hydrophobic | Pi-Alkyl | |
| C:VAL523 | 3.81626 | Hydrophobic | Pi-Alkyl | |
| C:ALA527 | 3.96014 | Hydrophobic | Pi-Alkyl | |
| C:LEU352 | 5.45723 | Hydrophobic | Pi-Alkyl | |
| C:ALA527 | 4.44987 | Hydrophobic | Pi-Alkyl | |
| VT12 | | | | -8.266 |
| C:VAL349 | 4.53718 | Hydrophobic | Pi-Alkyl | |
| C:ALA527 | 3.87976 | Hydrophobic | Pi-Alkyl | |
| C:ALA527 | 5.18297 | Hydrophobic | Pi-Alkyl | |
| C:LEU352 | 5.49986 | Hydrophobic | Pi-Alkyl | |
| C:VAL523 | 3.77329 | Hydrophobic | Pi-Alkyl | |
| VT13 | | | | -5.307 |
| C:LEU352 | 5.02138 | Hydrophobic | Pi-Alkyl | |
| C:ALA516 | 5.15123 | Hydrophobic | Pi-Alkyl | |
| C:VAL523 | 3.81626 | Hydrophobic | Pi-Alkyl | |
| C:VAL523 | 3.827 | Hydrophobic | Pi-Alkyl | |
| C:ALA527 | 3.96014 | Hydrophobic | Pi-Alkyl | |
| C:LEU352 | 5.45723 | Hydrophobic | Pi-Alkyl | |
| C:ALA527 | 4.44987 | Hydrophobic | Pi-Alkyl | |
| VT14 | | | | -8.706 |
| C:VAL349 | 4.30499 | Hydrophobic | Pi-Alkyl | |
| C:LEU352 | 5.47212 | Hydrophobic | Pi-Alkyl | |
| C:ALA527 | 5.25417 | Hydrophobic | Pi-Alkyl | |
| C:ALA527 | 3.89678 | Hydrophobic | Pi-Alkyl | |
| C:VAL523 | 3.75125 | Hydrophobic | Pi-Alkyl | |
| C:LEU93 | 4.675 | Hydrophobic | Pi-Alkyl | |
| C:VAL116 | 4.3717 | Hydrophobic | Pi-Alkyl | |

| Name | Distance | Category | Type | Docking score |
|---|---|---|---|---|
| VT15 | | | | -8.071 |
| C:TYR385 | 4.88974 | Electrostatic | Pi-Cation | |
| C:SER353:HA - | 2.43692 | Hydrophobic | Pi-Sigma | |
| C:TYR355 | 4.94992 | Hydrophobic | Pi-Pi T-shaped | |
| C:TYR355 | 5.32554 | Hydrophobic | Pi-Pi T-shaped | |
| C:TRP387 | 5.57571 | Hydrophobic | Pi-Pi T-shaped | |
| C:GLY526:C,O;ALA527:N | 4.55619 | Hydrophobic | Amide-Pi Stacked | |
| C:VAL116 | 4.41488 | Hydrophobic | Pi-Alkyl | |
| C:LEU359 | 5.21126 | Hydrophobic | Pi-Alkyl | |
| C:ALA527 | 5.45527 | Hydrophobic | Pi-Alkyl | |
| C:ALA527 | 3.98011 | Hydrophobic | Pi-Alkyl | |
| C:LEU352 | 5.24095 | Hydrophobic | Pi-Alkyl | |
| C:LEU352 | 5.49923 | Hydrophobic | Pi-Alkyl | |
| C:VAL523 | 3.66723 | Hydrophobic | Pi-Alkyl | |
| VT16 | | | | |
| C:ARG120:NH1 | 4.16804 | Electrostatic | Pi-Cation | -6.673 |
| C:MET522:SD | 5.47639 | Other | Pi-Sulfur | |
| C:MET522:SD | 4.71032 | Other | Pi-Sulfur | |
| C:PHE518 | 5.29557 | Hydrophobic | Pi-Pi Stacked | |
| C:PHE518 | 5.83535 | Hydrophobic | Pi-Pi Stacked | |
| C:TYR385 | 4.54697 | Hydrophobic | Pi-Pi T-shaped | |
| C:TRP387 | 4.89411 | Hydrophobic | Pi-Pi T-shaped | |
| C:GLY526:C,O;ALA527:N | 4.14783 | Hydrophobic | Amide-Pi Stacked | |
| C:GLY526:C,O;ALA527:N | 4.43424 | Hydrophobic | Amide-Pi Stacked | |
| C:LEU352 | 3.86365 | Hydrophobic | Alkyl | |
| C:LEU384 | 5.4755 | Hydrophobic | Pi-Alkyl | |
| C:VAL523 | 5.30304 | Hydrophobic | Pi-Alkyl | |
| C:ALA527 | 4.90706 | Hydrophobic | Pi-Alkyl | |
| C:VAL349 | 4.59191 | Hydrophobic | Pi-Alkyl | |
| C:ALA527 | 3.8049 | Hydrophobic | Pi-Alkyl | |
| C:LEU531 | 4.97249 | Hydrophobic | Pi-Alkyl | |

commonly used for data modelling. These look for relationships between a collection of chemical and structural molecules in question and certain property using statistical methods. Choosing appropriate mathematical method, appropriate chemical descriptors for ADMET endpoint, sizable enough collection of data pertaining with same endpoint for model validation are all essential components of effective prediction models for ADMET parameters. Recent developments in the prediction of ADME-related physicochemical qualities (like lipophilicity), ADME properties (like absorption), and toxicity problems (like drug-drug interactions) are discussed in this article see Table 3. During the next ten years or so, automated medium and HTS *in vitro* tests will be employed.

## DISCUSSION

All of the "compounds had molecular weights less than 500," according to data warrior results, suggesting that they will bind action site. All drugs had LogP below 5, which indicates excellent penetration and absorption across cell membranes. Table 1 provides specifics on the "binding energies and hydrogen bonds" of VT1-VT16. Furthermore, the dock score values of all the produced compounds ranged from -9.5 and -5.307 kcal/mol, suggesting their binding energies lower to benzimidazole, which has "binding energy" of 7.0 kcal/mol. Analogues with best interactions and far from zero auto dock score determined as best conformation. Both complexes' Ramachandran Plot RMSD plot analysis revealed that the VT7-protein complex had a stable trajectory for more research after achieving excellent stability

**Table 2:** **Rotatable bonds; H-bond acceptors; H-bond donors; Lipinski violations; Ghose violations; Veber violations; Egan violations and Muegge violations of Benzimidazole Derivatives.**

| Comp code | #Rotatable bonds | #H-bond acceptors | #H-bond donors | Lipinski #violations | Ghose #violations | Veber #violations | Egan #violations | Muegge #violations |
|---|---|---|---|---|---|---|---|---|
| VT1 | 7 | 6 | 2 | 1 | 0 | 1 | 1 | 1 |
| VT2 | 7 | 5 | 2 | 0 | 0 | 0 | 1 | 1 |
| VT3 | 8 | 6 | 2 | 1 | 0 | 1 | 1 | 2 |
| VT4 | 8 | 6 | 2 | 0 | 0 | 0 | 1 | 1 |
| VT5 | 7 | 7 | 2 | 1 | 0 | 1 | 1 | 2 |
| VT6 | 8 | 8 | 3 | 1 | 0 | 1 | 1 | 1 |
| VT7 | 7 | 5 | 3 | 1 | 0 | 1 | 1 | 2 |
| VT8 | 7 | 5 | 3 | 1 | 0 | 1 | 1 | 2 |
| VT9 | 7 | 6 | 2 | 0 | 0 | 0 | 1 | 1 |
| VT10 | 8 | 7 | 2 | 1 | 0 | 1 | 1 | 0 |
| VT11 | 7 | 5 | 2 | 0 | 0 | 0 | 1 | 1 |
| VT12 | 8 | 8 | 3 | 1 | 0 | 1 | 1 | 1 |
| VT13 | 7 | 5 | 2 | 0 | 0 | 0 | 1 | 1 |
| VT14 | 11 | 8 | 2 | 1 | 1 | 2 | 1 | 2 |
| VT15 | 7 | 5 | 2 | 0 | 0 | 0 | 1 | 1 |
| VT16 | 7 | 6 | 2 | 0 | 0 | 0 | 1 | 1 |

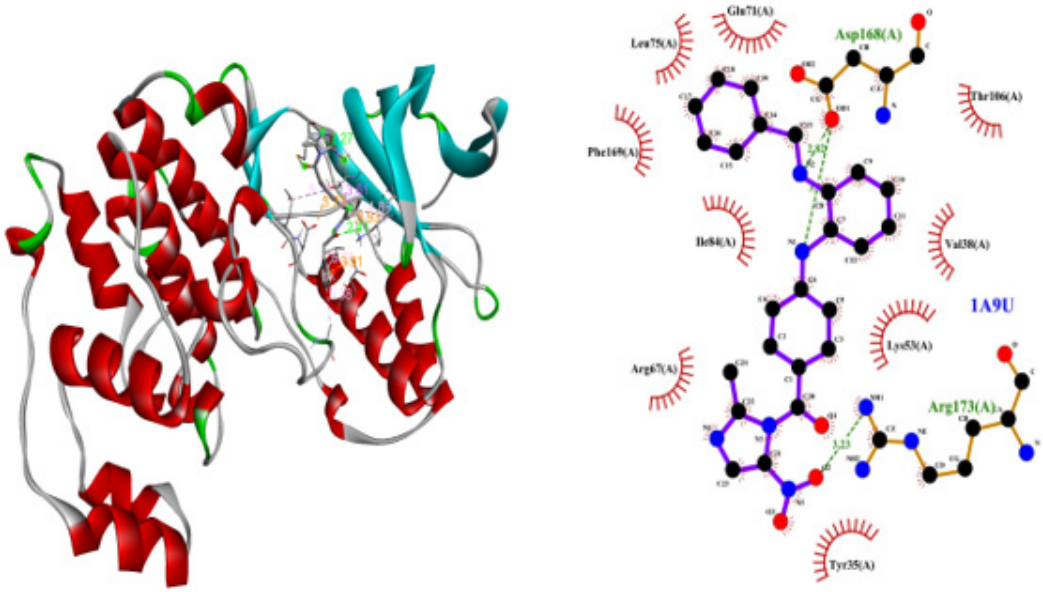


**Figure 3:** 2D and 3D conformations of the molecular bindings and Computer-Aided Molecular Design (CAMD) of VT 1.

at 100 ns. Analysis of the synthetic benzimidazole derivatives. Interactions towards COX-1 and COX-2 revealed that they have anti-inflammatory properties. Phe381, Leu-384, Tyr-385, Trp-387, Phe-518, Gly-526, Met-522, Tyr348, Val-349, Leu-352 were active amino acids in COX-1 (2OYE). VT5 and VT11 demonstrated Pi-Pi stacking to Tyr385 and Trp387 via the benzimidazole and H-bond with Ser-530 via nitrogen of the benzimidazole ring. VT6 demonstrated Pi-Pi stacking with Tyr385 via the benzimidazole ring and hydrogen bonding with Ser530. VT2 demonstrated Pi-Pi stacking with Tyr-385 via benzene ring and H-bond with Met-522 via nitrogen. Comparing the 16 benzimidazole derivatives to the standard domethacin (- 10.705 kcal/mol), VT8 and VT5 had a satisfactory docking score of -6.192 -7.668 kcal/mol. Phe381, Leu384, Tyr385, Trp387, were active amino acids in the enzyme COX-2 (4COX). VT5 demonstrated H-Bond with Ser-530 nitrogen of benzimidazole and Pi-Pi stacking with Tyr-385 via benzene. VT10 demonstrated Pi-cation interaction to Arg-120 via benzimidazole and Pi-pi stacking with Tyr-385

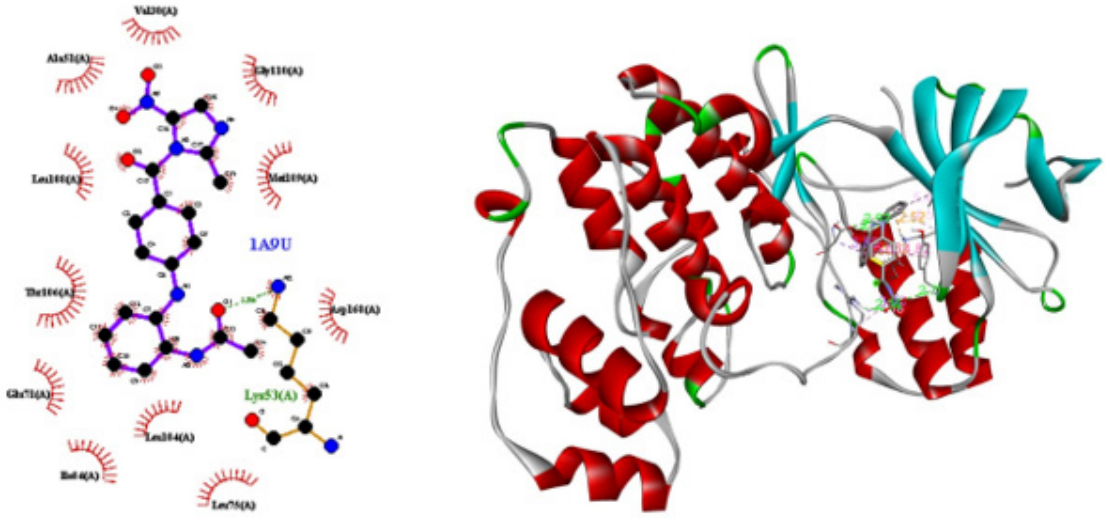


**Figure 4:** 2D and 3D conformations of the molecular bindings and Computer-Aided Molecular Design (CAMD) of VT 4.

**Table 3:** ***In silico*** **ADMET of Benzimidazole derivatives.**

| COMP. CODE | GI absorption | BBB permeant | Pgp substrate | CYP1A2 inhibitor | CYP2C19 inhibitor | CYP2C9 inhibitor | CYP2D6 inhibitor | CYP3A4 inhibitor | Bioavailability Score | PAINS #alerts |
|---|---|---|---|---|---|---|---|---|---|---|
| VT1 | Low | No | Yes | Yes | Yes | No | No | No | -5.87 | 0 |
| VT2 | Low | No | Yes | No | Yes | Yes | No | No | -4.43 | 0 |
| VT3 | Low | No | Yes | No | Yes | Yes | No | Yes | -4.71 | 0 |
| VT4 | Low | No | Yes | No | Yes | Yes | No | No | -5.07 | 0 |
| VT5 | Low | No | Yes | Yes | Yes | Yes | No | No | -5.21 | 0 |
| VT6 | Low | No | Yes | No | Yes | No | No | No | -7.49 | 0 |
| VT7 | Low | No | Yes | No | Yes | No | No | No | -5 | 1 |
| VT8 | Low | No | Yes | No | Yes | No | No | No | -5 | 0 |
| VT9 | Low | No | Yes | Yes | Yes | No | No | No | -5.03 | 0 |
| VT10 | Low | No | Yes | No | Yes | Yes | No | No | -5.78 | 0 |
| VT11 | Low | No | Yes | No | Yes | Yes | No | No | -4.43 | 0 |
| VT12 | Low | No | Yes | No | Yes | Yes | No | No | -7.03 | 0 |
| VT13 | Low | No | Yes | No | Yes | Yes | No | No | -4.43 | 0 |
| VT14 | Low | No | Yes | No | Yes | Yes | No | Yes | -5.12 | 0 |
| VT15 | Low | No | Yes | No | Yes | Yes | No | No | -4.98 | 0 |
| VT16 | Low | No | Yes | Yes | Yes | Yes | No | No | -4.81 | 0 |

and Trp-387 via benzene. VT9 demonstrated H-bond with Ser-530 via benzimidazole and Pi-Pi stacking with Tyr-385. Comparing 16 benzimidazole derivatives to the standard Indomethacin (-10.099 kcal/mol), VT5, VT6, VT2, and VT8 showed elevated docking scores, from -6.19 to -9.51 kcal/mol (Table 4). Compound VT5's binding affinity score with 2OYE is -56.79 kcal/mol, whereas compound VT2's binding score with 4COX is -60.27 kcal/mol. Late-stage drug attrition may now be decreased and the most promising compounds can be found using *in silico* ADME screens. To have a good *in vivo* response, pharmacodynamic and pharmacokinetic characteristics must be balanced. Further details on medication dose and regimen are also provided by ADMET. According to "Lipinski's rule of five", an oral medication is selected if its molecular weight is < 500, hydrogen bond donors is less than five, hydrogen bond acceptors is less than ten, and log *p* value less than five. Oral bioavailability depends on molecular flexibility, which is shown by the number of rotatable bonds. Additionally, as TPSA is indirectly related to percentage absorption, it suggested that used as 3D descriptor in number of hydrogen bonding groups. They should thus have

high oral absorption; nevertheless, this quality cannot be used to explain variances in bioactivity. Additionally, the compounds' oral absorption percentage ranged from 70.69 to 73.87%, indicating high ADME. Their TPSA values were 101.3 and 104.80 A2 (140 A2), respectively, and rotatable bonds ranged in 7 to 8 (<10). It is generally accepted that a molecule that is soluble in water and satisfies Lipinski's and Veber's criteria is said to possess both lipophilicity and hydrophilicity. Interactions towards COX-1 and COX-2 revealed that they have anti-inflammatory properties. Phe381, Leu-384, Tyr-385, Trp-387, Phe-518, Gly-526, Met-522, Tyr348, Val-349, Leu-352 were active amino acids in COX-1 (2OYE). VT1 and VT15 demonstrated Pi-Pi stacking to Tyr385 and Trp387 via the benzimidazole and H-bond with Ser-530 via nitrogen of the benzimidazole ring. VT12 demonstrated Pi-Pi stacking with Tyr385 via the benzimidazole ring and hydrogen bonding with Ser530. VT14 demonstrated Pi-Pi stacking with Tyr-385 via benzene ring and H-bond with Met-522 via nitrogen. Comparing the 16 benzimidazole derivatives to the standard Indomethacin (- 10.705 kcal/mol), VT14 and VT15 had a satisfactory docking score of -7.572 kcal/mol. Phe381, Leu384, Tyr385, Trp387, were active amino acids in the enzyme COX-2 (4COX). VT5 demonstrated H-Bond with Ser-530 nitrogen of benzimidazole and Pi-Pi stacking with Tyr-385 via benzene. VT10 demonstrated Pi-cation interaction to Arg-120 via benzimidazole and Pi-pi stacking with Tyr-385 and Trp-387 via benzene. VT9 demonstrated H-bond with Ser-530 via benzimidazole and Pi-Pi stacking with Tyr-385. Comparing 16 benzimidazole derivatives to the standard Indomethacin (-10.099 kcal/mol), VT14, VT15, VT2, and VT4 showed elevated docking scores, from -9.25 to -7.51 kcal/mol (Table 2). Compound VT5's binding affinity score with 2OYE is -56.79 kcal/mol, whereas compound VT2's binding score with 4COX is -60.27 kcal/mol. Late-stage drug attrition may now be decreased and the most promising compounds can be found using *in silico* ADME screens. To have a good *in vivo* response, pharmacodynamic and pharmacokinetic characteristics must be balanced. Further details on medication dose and regimen are also provided by ADMET.

## CONCLUSION

As a result, these *in silico* methods have helped identify binding and affinity between COX enzyme and benzimidazoles, responsible for anti-inflammatory properties. To ascertain their anti-inflammatory properties, benzimidazole analogues were docked with COX-1 (2OYE) and COX-2 (4COX). All of the compounds' values were discovered to be within the typical range, and Lipinski's rule of five was not broken. Therefore, it is anticipated that the compounds will have a high oral bioavailability. The ligands VT1 and VT4 had high docking scores with COX-2 (-9.492 kcal/mol) and COX-1 (-8.572 kcal/mol), respectively, out of the 16 benzimidazole derivatives. Furthermore, the pharmacophoric characteristics that underlie their biological action were also disclosed.

## ACKNOWLEDGEMENT

The authors are thankful to Dr. S.B. Bhawar, Pravara Rural College of Pharmacy, Pravaranagar.

## ABBREVIATIONS

**mg/kg:** Milligram/kilograms; **sec:** Seconds; **kcal:** Kilocalorie; **Mol.Wt:** Molecular Weight; **gm:** Gram; **LEU:** Leucine; **THR:** Threonine; **ALA:** Alanine; **MET:** Methionine; **PHE:** Phenylalanine; **COX:** Cyclooxygenase Enzyme; **WHO:** World health association; **Log P:** Partition coefficient.

## CONFLICT OF INTEREST

The authors declare that there is no conflict of interest.

## REFERENCES

Ayeni, E. A., Aldossary, A. M., Ayejoto, D. A., Gbadegesin, L. A., Alshehri, A. A., Alfassam, H. A., Afewerky, H. K., Almughem, F. A., Bello, S. M., & Tawfik, E. A. (2022). Neurodegenerative diseases: Implications of environmental and climatic influences on neurotransmitters and neuronal hormones activities. International Journal of Environmental Research and Public Health, 19(19), Article 12495. https://doi.org/10.3390/ijerph191912495

Bomalaski, M. N., Claflin, E. S., Townsend, W., & Peterson, M. D. (2017). Zolpidem for the treatment of neurologic disorders: A systematic review. JAMA Neurology, 74(9), 1130–1139. https://doi.org/10.1001/jamaneurol.2017.1133

Bortoli, M., Dalla Tiezza, M., Muraro, C., Pavan, C., Ribaudo, G., Rodighiero, A., Tubaro, C., Zagotto, G., & Orian, L. (2019). Psychiatric disorders and oxidative injury: Antioxidant effects of zolpidem therapy disclosed *in silico*. Computational and Structural Biotechnology Journal. PubMed, 17, 311–318. https://doi.org/10.1016/j.csbj.2, https://www.ncbi.nlm.nih.gov/pmc/articles/PMC6396081/

Chen, L., Deng, H., Cui, H., Fang, J., Zuo, Z., Deng, J., Li, Y., Wang, X., & Zhao, L. (2018). Inflammatory responses and inflammation-associated diseases in organs. Oncotarget. PubMed, 9(6), 7204–7218. https://doi.org/10.18632/oncotarget.23208, https://www.ncbi.nlm.nih.gov/pmc/articles/PMC5805548/

Das, S. N., & Chatterjee, S. (1995). Long-term toxicity study of ART-400. Indian Indg Med, 16(2), 117–123.

Durand, A., Thénot, J. P., Bianchetti, G., & Morselli, P. L. (1992). Comparative pharmacokinetic profile of two imidazopyridine drugs: Zolpidem and alpidem. Drug Metabolism Reviews, 24(2), 239–266. https://doi.org/10.3109/03602539208996294, https://pubmed.ncbi.nlm.nih.gov/1576937/

García-López, E. B., Muñoz-Ochoa, M., Hernández-Guerrero, C. J., Nieto-Camacho, A., & Band-Schmidt, C. J. (2021). Evaluation of anti-inflammatory activity of macroalgae collected from Baja California Sur, Mexico. International Journal of Pharmacy and Pharmaceutical Sciences, 13(8), 81–88. https://doi.org/10.22159/ijpps.2021v13i8.41453

García-Santos, G., Herrera, F., Martín, V., Rodriguez-Blanco, J., Antolín, I., Fernández-Marí, F., & Rodriguez, C. (2004). Antioxidant activity and neuroprotective effects of zolpidem and several synthesis intermediates. Free Radical Research, 38(12), 1289–1299. https://doi.org/10.1080/10715760400017343, https://pubmed.ncbi.nlm.nih.gov/15763953/

Hasanvand, A., Pirzadroozbahani, N., Ahmadizar, F., Kharazmkia, A., Mir, S., Amanolahi Baharvand, P. A., Goudarzi, M., & Mohammadrezaei Khorramabadi, R. (2018). Evaluation of the antioxidant effects of zolpidem in the rat model of cisplatin-induced nephrotoxicity. Journal of Renal Injury Prevention, 7(4), 235–239. https://doi.org/10.15171/jrip.2018.54

Hoehns, J. D., & Perry, P. J. (1993). Zolpidem: A nonbenzodiazepine hypnotic for treatment of insomnia. Clinical Pharmacy, 12(11), 814–828.

Holm, K. J., & Goa, K. L. (2000, April). Zolpidem: An update of its pharmacology, therapeutic efficacy and tolerability in the treatment of insomnia. Drugs, 59(4), 865–889. https://doi.org/10.2165/00003495-200059040-00014, https://pubmed.ncbi.nlm.nih.gov/10804040/

Jia, Z., Wang, P., Xu, Y., Feng, G., Wang, Q., He, X., Song, Y., Liu, P., & Chen, J. (2022). Trypsin inhibitor LH011 inhibited DSS-induced mice colitis via alleviating inflammation and oxidative stress. Frontiers in Pharmacology. PubMed, 13, Article 986510. https://doi. https://doi.org/10.3389/fphar.2022.986510, https://www.ncbi.nlm.nih.gov/pmc/articles/PMC9551103/

Lamptey, R. N. L., Chaulagain, B., Trivedi, R., Gothwal, A., Layek, B., & Singh, J. (2022). A review of the common neurodegenerative disorders: Current therapeutic approaches and the potential role of nanotherapeutics. International Journal of Molecular Sciences, 23(3), Article 1851. https://doi.org/10.3390/ijms23031851

Langtry, H. D., & Benfield, P. (1990). Zolpidem. A review of its pharmacodynamic and pharmacokinetic properties and therapeutic potential. Drugs, 40(2), 291–313. https://doi.org/10.2165/00003495-199040020-00008, https://pubmed.ncbi.nlm.nih.gov/2226217/

Miao, J., Ma, H., Yang, Y., Liao, Y., Lin, C., Zheng, J., Yu, M., & Lan, J. (2023). Microglia in Alzheimer's disease: Pathogenesis, mechanisms, and therapeutic potentials. Frontiers in Aging Neuroscience. PubMed, 15, Article 1201982. https://doi.org/10.3389/fn, https://www.ncbi.nlm.nih.gov/pmc/articles/PMC10309009/

**Cite this article:** Tawate VR, Tambe SK, Mankar SP, Wani NM, Vikhe SA, Sonawane MD, *et al*. Computational Tool and Molecular Properties to Identify the Molecular Targets of Novel Benzimidazole Derivatives as Potential COX Inhibitors via *in silico* Approaches. Int. J. Pharm. Investigation. 2026;16(2):654-66.